

DEEP-LEARNING-ASSISTED CONFIGURATION OF RECONFIGURABLE INTELLIGENT SURFACES IN DYNAMIC RICH-SCATTERING ENVIRONMENTS

Kyriakos Stylianopoulos, Nir Shlezinger, Philipp del Hougne, and George C. Alexandropoulos

ABSTRACT

The integration of Reconfigurable Intelligent Surfaces (RISs) into wireless environments endows channels with programmability, and is expected to play a key role in future communication standards. To date, most RIS-related efforts focus on quasi-free-space, where wireless channels are typically modeled analytically. Many realistic communication scenarios occur, however, in rich-scattering environments which, moreover, evolve dynamically. These conditions present a tremendous challenge in identifying an RIS configuration that optimizes the achievable communication rate. In this paper, we make a first step toward tackling this challenge. Based on a simulator that is faithful to the underlying wave physics, we train a deep neural network as surrogate forward model to capture the stochastic dependence of wireless channels on the RIS configuration under dynamic rich-scattering conditions. Subsequently, we use this model in combination with a genetic algorithm to identify RIS configurations optimizing the communication rate. We numerically demonstrate the ability of the proposed approach to tune RISs to improve the achievable rate in rich-scattering setups.

Index terms— Reconfigurable intelligent surfaces, deep learning, rich-scattering, dynamic wireless environments.

1. INTRODUCTION

Recent years have witnessed the emergence of programmable wireless environments, enabled by using Reconfigurable Intelligent Surfaces (RISs), as a disruptive new wireless networking paradigm [1–5]. Programmable wireless channels open up a host of new opportunities in wireless communications and sensing. The majority of RIS-based ideas has to date been explored under the assumption of quasi-free-space, possibly with a few known scatterers. These conditions enable the deployment of analytical channel models for wireless propagation. In practice, estimating the channels in RIS-aided communication is expected to be complex and costly [6–10].

The associated challenges become more complex when we turn to rich-scattering environments. Indoor environments

inside buildings, metro stations, and vessels or airplanes often act as irregularly shaped scattering enclosures that give rise to significant reverberation. Wave propagation under these rich-scattering conditions strongly differs from the intensely studied free-space case [4]. Previous works explored the optimization of communication-related metrics in RIS-enabled *static* rich-scattering enclosures [4, 11, 12], focusing on enforcing pulse-like channel impulse responses for simple modulation scenarios based on either iterative experimental optimization of the RIS [4, 11–13], or on the availability of channel state information [14, 15]. However, realistic rich-scattering environments are rarely static [16]. The motion of inhabitants, rotating fans, and other factors yield a *dynamic* nature of such environments that results in fast fading of the wireless channels, impacting communication design and limiting the ability to rely on channel knowledge.

In this paper, we make a first step toward tackling the challenge of identifying an RIS configuration that optimizes the communication rate in a dynamic rich-scattering environment. Given the overwhelming complexity of the rich-scattering environment, an analytical explicit treatment is intractable. Instead, our approach embraces the stochastic nature of the channel coefficients under such conditions. We capture the link between the RIS configuration and the key statistical parameter of the channel that determines the communication rate using a Deep Neural Network (DNN). Specifically, we use a low-Signal-to-Noise Ratio (SNR) approximation of the ergodic achievable rate in rich-scattering wireless channels, which can be computed from their statistical moments, i.e., using the output of the trained DNN. Based on this learned DNN model, we apply a genetic algorithm to optimize the RIS configuration in light of the ergodic capacity objective, inspired by the success of similar techniques in the context of deep priors [17, 18]. We numerically demonstrate that the proposed DNN-assisted optimization tunes the RIS to support rates within a minor gap of the maximal achievable values, without relying on explicit knowledge of the channel statistics and its interplay with the RIS setting.

2. SYSTEM MODEL

2.1. Channel Model

We consider a rich-scattering scenario in which a transmitter is communicating with a receiver inside an irregularly-shaped metallic enclosure that is equipped with an RIS. The channels exhibit rich-scattering due to reverberation inside the com-

K. Stylianopoulos and G. C. Alexandropoulos are with the Department of Informatics and Telecommunications, National and Kapodistrian University of Athens, 15784 Athens, Greece (e-mail: {kstylianop; alexandg}@di.uoa.gr). N. Shlezinger is with the School of ECE, Ben-Gurion University of the Negev, Beer-Sheva, Israel (e-mail: nirshl@bgu.ac.il). P. del Hougne is with Univ Rennes, CNRS, IETR - UMR 6164, F-35000, Rennes, France (e-mail: philipp.del-hougne@univ-rennes1.fr). The work was supported by the EU H2020 RISE-6G project under grant number 101017011.

plex scattering enclosure resulting in multiple reflections off the walls. A perturbing object rotates in an uncontrolled manner inside the environment, yielding the dynamic nature of the fading wireless channel [16]. The RIS is comprised of N reflecting elements, where each element can take values in a set \mathcal{S} representing the possible states one can configure. Since RISs typically admit a finite number of configurations, e.g., when controlled via PIN diodes [11, 12, 19], we assume that \mathcal{S} is finite (specifically, binary), and denote the overall configuration of the RIS by the vector $\varphi \in \mathcal{S}^N$.

The channel perturbations are assumed to be sufficiently fast to interpret the input-output relationship as a fast-fading frequency-selective channel in discrete time. Let $h(t)$ be the stochastic channel impulse response, encapsulating both rays traversing via the RIS as well as those which do not encounter it. While the statistics of $h(t)$ are affected by the RIS setting φ , this dependence may be extremely complex and even intractable [4]. Letting $y(t)$ be the channel output observed by the receiver, the input-output relationship can be expressed as:

$$y(t) = h(t) * x(t) + w(t), \quad t \in \mathbb{Z}, \quad (1)$$

where $*$ is the convolution operator, $x(t)$ is the channel input, and $w(t)$ is the white Gaussian noise with variance σ^2 . We assume that the transmission bandwidth is divided into B bins, not smaller than the coherence bandwidth, with central frequencies f_1, f_2, \dots, f_B , and use $\{\rho(f_i)\}_{i=1}^B$ to denote the input spectral power allocation. Our DNN approach's training data is obtained from a simulator that faithfully represents the wave physics of the underlying rich-scattering scenario [16]; the channel model and simulator are detailed in [20].

2.2. Problem Formulation

Our goal is to design a scheme for tuning the RIS configuration φ for a given input spectral power allocation $\{\rho(f_i)\}_{i=1}^B$ in order to maximize the rate of achievable reliable communications. As the channel is fast-fading, we aim to maximize the ergodic achievable rate, given by [21, Ch. 4.3] as

$$R(\varphi) \triangleq \mathbb{E}_{\{H(f_i)\}_{i=1}^B} \left\{ \sum_{i=1}^B \log_2 \left(1 + \frac{|H(f_i)|^2 \rho(f_i)}{\sigma^2} \right) \right\}, \quad (2)$$

where $H(f) \triangleq \mathcal{F}\{h(t)\}$ is the stochastic channel frequency response between the single-antenna transmitter and receiver at frequency bin f , whose statistics depend on φ , while $\mathcal{F}(\cdot)$ is the discrete Fourier transform with B bins. While the explicit relationship between the channel frequency response and a specific RIS configuration is unknown, extremely complex, and dependent on the perturber orientation, we have access to a training set of channels and their corresponding configuration, i.e., to T pairs of the form $\{\varphi_t, \{H_t(f_i)\}_{i=1}^B\}_{t=1}^T$.

3. RIS CONFIGURATION METHODS

3.1. Rationale

Determining the RIS configuration which maximizes the ergodic rate in (2) is associated with two core challenges:

1) computing the stochastic expectation with respect to the distribution of $\{H(f_i)\}_{i=1}^B$; and 2) identifying the relationship between the RIS configuration φ and the distribution of $\{H(f_i)\}_{i=1}^B$. Neither of these tasks appears to be solvable with an analytical model of the wireless channels.

To address the first challenge, we use a low-SNR approximation of the ergodic rate as our RIS-optimization objective:

$$\tilde{R}(\varphi) \triangleq \sum_{i=1}^B \log_2 \left(1 + \frac{\mathbb{E}\{|H(f_i)|^2\} \rho(f_i)}{\sigma^2} \right). \quad (3)$$

The objective (3) only requires a characterization of the relationship between φ and the second-order moments of the channel frequency responses. To tackle the second challenge, we train a dedicated DNN which maps φ to the second-order moments of the channel frequency responses. Ultimately, we will utilize this DNN to find the RIS configuration which optimizes (3) using Genetic Algorithms (GAs), as detailed next.

3.2. Optimizing RIS Configuration

Our proposed method for optimizing the RIS configuration based on the objective (3) consists of two components: A DNN which learns to capture the relationship between φ and $\mathbf{m} \triangleq [\mathbb{E}\{|H(f_1)|^2\}, \mathbb{E}\{|H(f_2)|^2\}, \dots, \mathbb{E}\{|H(f_B)|^2\}]$; and a GA using the DNN for optimizing the RIS configuration.

RIS-Channel DNN: In order to learn how to map φ into an estimate of \mathbf{m} , we use a regression DNN whose exact architecture is described in Section 4. In order to learn the parameters of the DNN, denoted by θ , we first cluster the available data $\{\varphi_t, \{H_t(f_i)\}_{i=1}^B\}_{t=1}^T$ into $C \leq |\mathcal{S}|^N$ clusters based on the RIS setting φ_t . For each cluster of index $c = 1, 2, \dots, C$, we estimate $\{\mathbb{E}\{|H(f_i)|^2\}\}_{i=1}^B$ by averaging over the squared magnitude of the corresponding measured channels into the vector $\hat{\mathbf{m}}_c \in \mathcal{R}_+^B$. The resulting dataset, denoted by $\mathcal{D} \triangleq \{\varphi_c, \hat{\mathbf{m}}_c\}_{c=1}^C$, is used for training the DNN based on the Mean Squared Error (MSE) loss function with an added ℓ_2 -regularization term to avoid overfitting, i.e.:

$$\mathcal{L}(\theta) = \sum_{c=1}^C \|\hat{\mathbf{m}}_\theta(\varphi_c) - \hat{\mathbf{m}}_c\|^2 + \lambda \|\theta\|^2. \quad (4)$$

In (4), $\hat{\mathbf{m}}_\theta(\cdot)$ denotes the DNN mapping with parameters θ , and λ is the regularization factor.

Optimizing φ : Once the DNN is trained, we use it to determine the setting φ that maximizes (3) by approximating $\{\mathbb{E}\{|H(f_i)|^2\}\}_{i=1}^B$ with the network's prediction $\hat{\mathbf{m}}_\theta(\cdot)$. Since φ takes values in the discrete set \mathcal{S}^N , we do so using discrete optimization. We employ a GA, which is described in the sequel for binary configurations (i.e., $|\mathcal{S}| = 2$), corresponding to the RIS considered in Section 4 in line with current experimental prototypes [4, 11–13, 19]. However, the algorithm can be adapted to any finite $|\mathcal{S}|$ in the same manner, since GA is applicable to arbitrary discrete optimization [22].

At every iteration (*generation*) of index k , the GA maintains a set (*population*) $\mathcal{P}^{(k)}$ of size l_{pop} with candidate RIS

Algorithm 1: Proposed Deep RIS Setting

Data: Dataset $\mathcal{D} = \{\varphi_c, \hat{\mathbf{m}}_c\}_{c=1}^C, k_{\max}$, and l_{pop} .

- 1 Train DNN using \mathcal{D} based on loss (4) to obtain θ .
- 2 Randomly initialize population $\mathcal{P}^{(1)} = \{\varphi_j^{(1)}\}_{j=1}^{l_{\text{pop}}}$.
- 3 Set $s_{\max} = -\infty$ and $\varphi_{\max} = \emptyset$.
- 4 **for** $k = 1, 2, \dots, k_{\max}$ **do**
- 5 **for** $j = 1, 2, \dots, l_{\text{pop}}$ **do**
- 6 Calculate $\tilde{R}(\varphi_j^{(k)})$ from (3) using $\hat{\mathbf{m}}_{\theta}(\varphi_j^{(k)})$.
- 7 Set score $s_j^{(k)} = \tilde{R}(\varphi_j^{(k)})$.
- 8 **if** $s_j^{(k)} > s_{\max}$ **then**
- 9 Set $s_{\max} = s_j^{(k)}$ and $\varphi_{\max} = \varphi_j^{(k)}$.
- 10 **end**
- 11 **end**
- 12 Generate $\mathcal{P}^{(k+1)}$ from $\mathcal{P}^{(k)}$ using $\{s_j^{(k)}\}_{j=1}^{l_{\text{pop}}}$.
- 13 **end**

Output: RIS configuration φ_{\max} .

configurations (*solutions*), which are used for evaluating the objective (*fitness*) function, i.e., (3). The next generation is then determined by the current population's *offspring*, which is produced by applying the following steps in sequence:

1. *Tournament selection*: A multi-set, with length l_{pop} , of *parent* solutions is created by repeating the following process for each element: k_{tour} solutions from the current generation are sampled with replacement to participate. The solution with the highest fitness score is selected as a parent.
2. *Uniform crossover*: The crossover mechanism involves creating two new candidate solution-vectors (*offspring*) by combining information from candidates of the past generation (*parents*). Parents are assigned to pairs randomly. For each pair, two offspring solutions are generated. The first is constructed by selecting each bit from either parent with equal probability, and the latter as its ones-complement.
3. *Flip-bit mutation*: Each offspring solution has each of its bits flipped with probability p_{mut} .

The above procedure results in an updated generation of equal size l_{pop} . The optimization is accomplished due to the fact that, solutions with high fitness scores participate in the evolutionary process to exchange genetic information, while the imposed stochasticity in all three steps leads to efficient exploration of the search space. As a standard practice, the solution with the maximum fitness score discovered at any generation is kept at the end. The resulting Deep RIS Setting algorithm steps are summarized in Algorithm 1.

3.3. Discussion

Algorithm 1 enables the optimization of the RIS configuration under fast-fading frequency selective channels, such as those arising in rich-scattering conditions. It bypasses the need to impose a model on the relationship between the RIS configuration and the channel frequency response, in a manner

amenable to discrete optimization using deep learning techniques. As opposed to [4], where DNNs were trained to capture the instantaneous channel realization, here we account for the inherent stochasticity of rich-scattering channels and design our DNN to estimate their statistical moments. Note that the DNN does not try to learn the ergodic rate directly, even though it is the metric we ultimately try to optimize. This was decided because rate calculations are dependent on noise and spectral allocation values, hence, having a DNN estimating the ergodic rate would imply that it would have to be retrained multiple times in setups of varying characteristics.

Our current formulation considers a scalar point-to-point channel, and does not account for possible side information arising from, e.g., knowledge of the location of the communicating devices. When such additional knowledge is present, one can potentially incorporate it into the RIS-channel DNN as a form of a hypernetwork [23]. Furthermore, Algorithm 1 can also be extended to multi-user and multi-antenna systems, by, e.g., replacing the ergodic rate objective with the ergodic sum-rate for either uplink or downlink systems. Finally, our derivation of Algorithm 1 considers a fixed input power allocation $\rho(f)$. One can utilize the proposed approach to also optimize $\rho(f)$ in a joint manner with the RIS configuration. We leave the aforementioned extensions for future work.

4. NUMERICAL RESULTS

We now apply our proposed method in a numerical study¹. To that aim, we have simulated a rich-scattering environment with a single-antenna access point, a fixed-position and single-antenna Receiver (RX), and an RIS consisting of $N = 21$ binary-tunable elements. We selected on purpose a relatively “small” number of possible RIS configurations (i.e., 2^{21}), because they can be scanned with an exhaustive search, so that we can identify the globally optimal RIS configuration for rate maximization. To generate the rich-scattering environment, we have developed a simulator based on [16, 20], simulating a rotating object that perturbs the environment. The transmission observed at the RX has been evaluated over $B = 30$ frequency bins.

The data preparation step involves attaining mean frequency response measurements for different RIS profiles, as described in Section 3.2. At first, $C = 500$ RIS configurations, $\{\varphi_c\}_{c=1}^C$, were randomly selected. For each φ_c , we have set the perturber orientation to 100 random angles, thus generating stochastic $\{H(f_i)\}_{i=1}^B$ measurements, which were then averaged out (per frequency point) to produce the target vectors $\hat{\mathbf{m}}_c$. Finally, \mathcal{D} was constructed as $\{\varphi_c, \hat{\mathbf{m}}_c\}_{c=1}^C$ and we allocated 80% of the data to the training set, whereas the remaining set was split in half to validation and test subsets.

The RIS-channel DNN is comprised of two fully connected hidden layers of 64 units, each with ReLU activations.

¹The paper's TensorFlow code and used data are available at: https://github.com/NoesysLab/Deep_RIS_Tuning_for_Rich_Scattering_Environments.

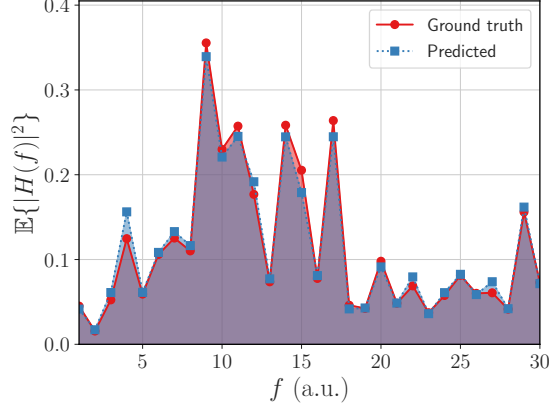


Fig. 1. Ground truth and predicted mean frequency response of a random RIS configuration on which the network has not been trained. The frequency points are in arbitrary units (a.u.).

The output layer has B neurons with linear activation to facilitate the regression process. Since the size of the data set is relatively small, we have set the regularization factor to $\lambda = 2.5 \times 10^{-5}$, and trained using Adam [24] with a learning rate of 0.001. The hyper-parameter values for the learning rate, number of layers, units, and regularization factor were selected through grid search over possible combinations as the ones that minimize the MSE of the validation set. The model was trained using early stopping, based on the validation MSE, for a total of 883 epochs. The resulting MSE of the trained model on the test set was 1.27×10^{-4} , which signifies that the network was indeed capable of learning channel statistics even in rich-scattering environments. To illustrate the DNN accuracy, the true and predicted squared magnitudes over the $B = 30$ bins for a random RIS profile are illustrated in Fig. 1. Clearly, the trained DNN succeeds in capturing the second-order moments of the channel frequency response.

Having trained and evaluated the RIS-channel DNN, we proceed to apply Algorithm 1 in order to identify a φ that maximizes the ergodic rate in (3). Apart from Algorithm 1, we consider the baseline of selecting the best out of 5000 randomly evaluated candidates (Top random). Furthermore, a lower and an upper bound are reported, which are constructed by taking the average rate out of the 5000 random configurations (Average) and by exhaustively evaluating all RIS configurations (Exhaustive). By setting the power allocation $\rho(f)$ to unity at all frequencies, we compare the achievable rates of the above methods versus the SNR. To obtain appropriate hyper-parameter values for our GA, a short grid search was implemented for determining the values of l_{pop} , k_{tour} , and p_{mut} . Since the action space was finite, allowing for a vast examination would be amenable to exhaustive search. Therefore, we allocated 30000 evaluations to search between 60 possible parameter combinations. The ones with the best performance were kept and the final algorithm was executed for 20000 evaluations (i.e., $20000/l_{\text{pop}}$ generations).

The achieved performances are plotted in Fig. 2, whereas

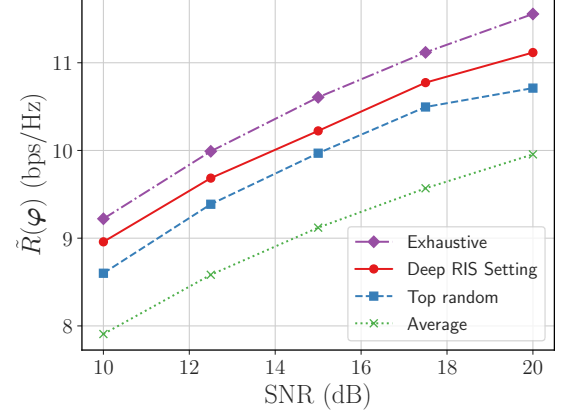


Fig. 2. Ergodic rate performance of the proposed method and baselines over different SNR values.

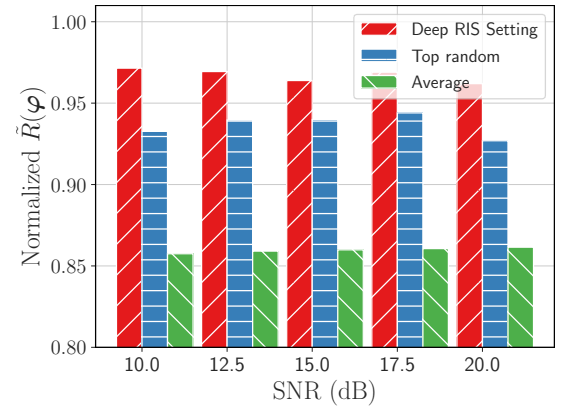


Fig. 3. Ergodic rate of the proposed method as a fraction of the optimal achievable rates of exhaustive search.

a normalized presentation, produced by dividing by the maximal achievable rate (via exhaustive search), is given in Fig. 3. It is shown that Algorithm 1, which adopts a DNN-aided GA, is capable of providing consistent improvements over the considered baselines. While the improvement offered by Algorithm 1 over the Top random strategy is approximately 1 dB in SNR, the margin for improvement in the studied scenario is limited *a priori*. This is illustrated by the facts that: (i) the optimal rate is only 15% greater than the random, and (ii) our proposed method performs close to the optimal performance.

5. CONCLUSION

In this paper, considering dynamic rich-scattering environments, we presented an RIS configuration algorithm which bypasses the need to analytically model or experimentally measure the relationship between the RIS and channel statistics, and instead learns it from data. Based on a low-SNR approximation of the ergodic rate, this learned model is then combined with a GA to optimize the RIS phase configuration. Our numerical study demonstrates the capability of our methodology to tune an RISs to boost reliable communications in dynamic rich-scattering environments.

6. REFERENCES

- [1] L. Subrt and P. Pechac, "Intelligent walls as autonomous parts of smart indoor environments," *IET Commun.*, vol. 6, no. 8, pp. 1004–1010, 2012.
- [2] C. Huang, A. Zappone, G. C. Alexandropoulos, M. Debbah, and C. Yuen, "Reconfigurable intelligent surfaces for energy efficiency in wireless communication," *IEEE Trans. Wireless Commun.*, vol. 18, no. 8, pp. 4157–4170, Aug. 2019.
- [3] M. Di Renzo *et al.*, "Smart radio environments empowered by reconfigurable AI meta-surfaces: An idea whose time has come," *EURASIP J. Wirel. Commun. Net.*, vol. 2019, no. 1, pp. 1–20, May 2019.
- [4] G. C. Alexandropoulos, N. Shlezinger, and P. del Hougne, "Reconfigurable intelligent surfaces for rich scattering wireless communications: Recent experiments, challenges, and opportunities," *IEEE Commun. Mag.*, vol. 59, no. 6, pp. 28–34, 2021.
- [5] E. Calvanese Strinati, G. C. Alexandropoulos, H. Wymeersch, B. Denis, V. Sciancalepore, R. D'Errico, A. Clemente, D.-T. Phan-Huy, E. D. Carvalho, and P. Popovski, "Reconfigurable, intelligent, and sustainable wireless environments for 6G smart connectivity," *IEEE Commun. Mag.*, vol. 59, no. 10, pp. 99–105, Oct. 2021.
- [6] Z. Wang, L. Liu, and S. Cui, "Channel estimation for intelligent reflecting surface assisted multiuser communications: Framework, algorithms, and analysis," *IEEE Trans. Wireless Commun.*, vol. 19, no. 10, pp. 6607–6620, Oct. 2020.
- [7] H. Liu, X. Yuan, and Y.-J. A. Zhang, "Matrix-calibration-based cascaded channel estimation for reconfigurable intelligent surface assisted multiuser MIMO," *IEEE J. Sel. Areas Commun.*, vol. 38, no. 11, pp. 2621–2636, Nov. 2020.
- [8] C. Hu, L. Dai, S. Han, and X. Wang, "Two-timescale channel estimation for reconfigurable intelligent surface aided wireless communications," *IEEE Trans. Commun.*, to appear, 2021.
- [9] G. C. Alexandropoulos, N. Shlezinger, I. Alamzadeh, M. F. Imani, H. Zhang, and Y. C. Eldar, "Hybrid reconfigurable intelligent metasurfaces: Enabling simultaneous tunable reflections and sensing for 6G wireless communications," *arXiv preprint: 2104.04690*, 2021.
- [10] S. Lin *et al.*, "Adaptive transmission for reconfigurable intelligent surface-assisted OFDM wireless communications," *IEEE J. Sel. Areas Commun.*, vol. 38, no. 11, pp. 2653–2665, Nov. 2020.
- [11] P. del Hougne, F. Lemoult, M. Fink, and G. Lerosey, "Spatiotemporal wave front shaping in a microwave cavity," *Phys. Rev. Lett.*, vol. 117, no. 13, p. 134302, 2016.
- [12] P. del Hougne, M. Fink, and G. Lerosey, "Optimally diverse communication channels in disordered environments with tuned randomness," *Nat. Electron.*, vol. 2, no. 1, pp. 36–41, 2019.
- [13] R. Zhou, X. Chen, W. Tang, X. Li, S. Jin, E. Basar, Q. Cheng, and T. J. Cui, "Modeling and measurements for multi-path mitigation with reconfigurable intelligent surfaces," *arXiv preprint: 2109.11820*, 2021.
- [14] E. Arslan, I. Yildirim, F. Kilinc, and E. Basar, "Over-the-air equalization with reconfigurable intelligent surfaces," *arXiv preprint: 2106.07996*, 2021.
- [15] H. Zhang, L. Song, Z. Han, and H. V. Poor, "Spatial equalization before reception: Reconfigurable intelligent surfaces for multi-path mitigation," in *Proc. IEEE ICASSP*, 2021, pp. 8062–8066.
- [16] P. del Hougne, "Robust position sensing with wave fingerprints in dynamic complex propagation environments," *Phys. Rev. Research*, vol. 2, no. 4, p. 043224, 2020.
- [17] A. Bora, A. Jalal, E. Price, and A. G. Dimakis, "Compressed sensing using generative models," in *Proc. Int. Conf. Mach. Lear.*, Sydney, Australia, Aug. 2017, pp. 537–546.
- [18] N. Shlezinger, J. Whang, Y. C. Eldar, and A. G. Dimakis, "Model-based deep learning," *arXiv preprint: 2012.08405*, 2020.
- [19] L. Dai, B. Wang, M. Wang, X. Yang, J. Tan, S. Bi, S. Xu, F. Yang, Z. Chen, M. Di Renzo *et al.*, "Reconfigurable intelligent surface-based wireless communications: Antenna design, prototyping, and experimental results," *IEEE Access*, vol. 8, pp. 45 913–45 923, 2020.
- [20] R. Faqiri, C. Saigre-Tardif, G. C. Alexandropoulos, N. Shlezinger, M. F. Imani, and P. del Hougne, "PhysFad: Physics-based end-to-end channel modeling of RIS-parametrized environments with adjustable fading," *arXiv preprint: 2202.02673*, 2022.
- [21] A. Goldsmith, *Wireless Communications*. Cambridge University Press, 2005.
- [22] M. Mitchell, *An Introduction to Genetic Algorithms*. Cambridge, MA, USA: MIT Press, 1998.
- [23] D. Ha, A. Dai, and Q. V. Le, "Hypernetworks," *arXiv preprint: 1609.09106*, 2016.
- [24] D. P. Kingma and J. Ba, "Adam: A method for stochastic optimization," *arXiv preprint: 1412.6980*, 2015.